International Journal of Mathematical, Engineering and Management Sciences
Vol. 10, No. 5, 1518-1538, 2025
https://doi.org/10.33889/IJMEMS.2025.10.5.072

Ram Arti Publishers

Analysis of Beams with a Three-dimensional Random Field of the Modulus of Elasticity Using the Stochastic Finite Element Method

Nguyen Dang Diem
Faculty of Civil Engineering, Campus in Ho Chi Minh City,
University of Transport and Communications, Ho Chi Minh City, Vietnam.
E-mail: diemnd_ph@utc.edu.vn

Pham Van Dat
Faculty of Civil Engineering, Hanoi Architectural University,
Km10 Nguyen Trai Street, Thanh Xuan District, Hanoi, Vietnam.
E-mail: datpv@hau.edu.vn

Ta Duy Hien
Faculty of Civil Engineering, University of Transport and Communications, Hanoi, Vietnam.
Corresponding author: tdhien@utc.edu.vn

(Received on January 1, 2025; Revised on March 13, 2025 & May 7, 2025; Accepted on May 21, 2025)

Abstract
This study proposes a stochastic finite element method (SFEM) for analyzing the static response of beams with material properties modeled as three-dimensional spatial random fields. The method employs weighted integration to discretize spatial variations in Young's modulus and utilizes a perturbation approach for efficient statistical response computation. Validation is performed using Monte Carlo simulations (MCs) with the spectral representation method to establish a benchmark dataset, showing strong agreement between the two methods, particularly for large correlation distances. The results demonstrate that spatial variability in Young's modulus significantly affects beam displacement. Shorter correlation lengths reduce displacement variability, while longer correlation lengths lead to greater deflection dispersion. Additionally, an enhancement in the standard deviation of Young's elastic modulus correlates with a higher coefficient of variation (COV) of displacement, confirming structural sensitivity to material randomness. The COV of displacement shows a nearly proportional relationship to the COV of Young's modulus, which provides key insights into the predictability of stochastic structural behavior. While SFEM is computationally more efficient than MCs, its first-order perturbation formulation limits accuracy in highly nonlinear cases. Future work should explore higher-order stochastic approximations, non-Gaussian random fields, and nonlinear extensions. These findings contribute to advancing stochastic structural analysis by extending SFEM to 3D random fields, providing a foundation for uncertainty quantification in engineering design and highlighting the importance of spatially varying material properties.

Keywords- SFEM, Three-dimensional, Random field, Beams, Weighted integration.

1. Introduction

Systems of partial differential equations, subject to boundary and initial conditions, mathematically model structural analysis problems involving loads and other excitations (Zhao et al., 2024). Analytical methods have been traditionally used to solve these equations by seeking their exact solutions. However, due to the mathematical complexity of these equations, analytical solutions can be challenging and computationally expensive. With the advent of high-speed electronic computers, the finite element method (FEM) has emerged as a powerful numerical technique for discretizing and solving complex structural analysis problems (Danh, 2024; Häussler-Combe, 2022; Talib, 2024). Input parameters such as loads, material properties, and geometric dimensions, often associated with uncertainties, are modeled as stochastic variables or fields (Wang et al., 2024). When such uncertainties are present, the governing differential equations become stochastic differential equations. The standard FEM being a deterministic method, is not directly applicable to these equations. The stochastic finite element method (SFEM), which combines the FEM with probabilistic concepts, provides a robust framework for investigating structures in the presence of stochastic variations (Cao et al., 2024; Huang et al., 2024; Huo et al., 2024). SFEM has found widespread applications in various fields, including materials science, biomechanics, geotechnical engineering, and general engineering.

The SFEM plays a crucial role in structural engineering, particularly in scenarios where uncertainties in material properties, loading conditions, and geometric imperfections significantly influence structural performance. In practical applications, SFEM is widely utilized for reliability assessment, enabling engineers to quantify the probability of failure due to material randomness, which is essential for infrastructure systems such as bridges, high-rise buildings, and offshore structures (Schuëller & Pradlwarter, 2007). Additionally, SFEM contributes to structural health monitoring by incorporating stochastic material degradation models to predict long-term performance under environmental and fatigue effects (Elishakoff & Ren, 2003; Stefanou, 2009). In aerospace and automotive engineering, where lightweight and high-performance structures are employed, SFEM facilitates the evaluation of stiffness, vibration characteristics, and failure probability in the presence of material variability (Arregui-Mena et al., 2016; Huang et al., 2024). Moreover, in geotechnical and earthquake engineering, SFEM is indispensable for modeling the stochastic behavior of soil properties, foundation materials, and seismic ground motion, thereby enhancing the resilience of structural systems (Popescu et al., 2005; Zhao et al., 2024). Beyond traditional engineering fields, SFEM has also found applications in bioengineering and composite materials, where it aids in analyzing the variability in mechanical properties of biological tissues and advanced composites (Huo et al., 2024; Nguyen et al., 2017).

Stochastic structural analysis within the framework of the SFEM involves several primary steps: (1) representing random input variables as Gaussian or non-Gaussian random fields; (2) discretizing random fields into random variables within the FEM framework; and (3) propagating random variables into the system and analyzing the structure's stochastic response. Common methods for representing Gaussian input stochastic fields include the turning bands method (TBM), spectral representation method, optimal linear estimation (OLE), Karhunen-Loève (K-L) expansion, and expansion optimal linear estimation (EOLE) methods (Stefanou, 2009). For non-Gaussian random fields, techniques that generate distribution of signal power over frequency functions consistent with the fundamental statistical characteristics of the field with spatial randomness (Gurley et al., 1997) or methods generating target random fields consistent with marginal probability distribution functions are commonly applied (Popescu et al., 2005). Within the SFEM framework, random fields are discretized into random variables through discretization methods proposed and developed by researchers. Typical random field discretization methods include nodal discretization methods. Stochastic fields are discretized into uncertain quantities through the values of the random field at several points within the element (Liu et al., 1986). Random fields can be discretized into random variables using average-based methods that involve integration across element domains. Depending on different discretization techniques, there are different names, such as the mean discretization method (Chakraborty & Bhattacharyya, 2002; Van den Nieuwenhof & Coyette, 2003) and the weighted integral discretization method (Deodatis, 1991; Hien, 2020). The final group of methods for discretizing random fields is the series expansion method. This method represents the stochastic field as a finite sum of eigenfunctions with coefficients being random variables (Grigoriu, 1993; Li et al., 2006; Zhang & Ellingwood, 1994). To propagate randomness into the system and analyze the stochastic response of the structure, various variants of SFEM have been developed. These methods are classified into three main groups: perturbation-based SFEM (Elishakoff & Ren, 2003), spectral representation-based SFEM (Nouy, 2009), and Monte Carlo simulation (MCs)-based SFEM (Schuëller & Pradlwarter, 2007, 2009; Thuan & Hien, 2021). Perturbation-based SFEM is suitable for problems with random input variables with small deviations, and this technique can be applied to linear and nonlinear analysis as well as eigenvalue analysis problems (Arregui-Mena et al., 2016). Meanwhile, spectral representation-based SFEM is suitable for linear analysis problems, while nonlinear analysis remains an open problem (Nouy, 2009). MCs-based SFEM is a direct method for stochastic structural analysis based on conventional statistical principles. However, problems with a large number of elements and dimensions require significant computational time and resources (Liu et al., 2022) . Usually, MCs-based SFEM is used as a method to verify the results of stochastic analysis using perturbation-based SFEM or spectral representation-based SFEM. The choice of random field representation and discretization technique affects the accuracy of the problem, while the choice of method for propagating randomness and analyzing the stochastic response of the structure determines the computational cost and time (Koh & Cirak, 2023).

SFEM plays a crucial role in beam analysis due to the inherent uncertainties in material properties and external loading conditions. In practice, beams are widely utilized in civil, mechanical, and aerospace structures and often exhibit spatially varying Young's modulus due to manufacturing imperfections, material aging, and environmental exposure (Cao et al., 2024; Chakraborty & Bhattacharyya, 2002). Such stochastic variations influence the overall stiffness of the structure, leading to discrepancies in mechanical responses. Additionally, beams are subjected to uncertain loads, including wind, seismic forces, and variable traffic loads in bridges, necessitating a stochastic approach for accurate structural response evaluation (Hien et al., 2019; Van Thuan & Chun, 2019). SFEM enables the probabilistic modeling of these uncertainties, providing precise assessments of displacement, stress distributions, and critical loads. By establishing a direct correlation between the stochastic variability of Young's modulus and structural response deviations, SFEM facilitates design optimization, enhances reliability, and mitigates risks in structural engineering and design (Johnson et al., 1997; Ren et al., 1997).

The stochastic response of beams subjected to random excitations has been a major research focus in recent years due to the growing demand for reliability-based design. Deodatis (1991) pioneered the weighted integration method to discretize stochastic fields and construct random stiffness matrices, laying the groundwork for subsequent SFEM studies. Perturbation-based SFEM has been extensively employed to assess randomness in structural frames, particularly under independent and dependent random field assumptions (Deodatis, 1990). Analytical solutions, such as those derived by Elishakoff et al. (1995), provide exact solutions for beams with randomly varying stiffness. However, due to the high mathematical complexity, these solutions are often limited to simplified problems. Ren et al. (1997) introduced a variational finite element approach to improve computational efficiency in uncertainty quantification, while the Karhunen–Loève (K-L) expansion has been widely adopted to reduce high-dimensional stochastic fields (Larsen et al., 2021). These methodologies optimize stochastic simulations, minimize computational costs, and maintain accuracy in structural analysis.

Recent studies have integrated SFEM with advanced computational techniques to develop more accurate stochastic stiffness models. Adhikari & Mukherjee (2022) combined Castigliano's theorem (Friedman & Kosmatka, 1993) with the K-L expansion to model beams with spatially varying material properties, enabling refined uncertainty quantification in practical engineering applications. Hien et al. (2019) MCs with spectral representation methods to analyze beam structures subjected to stochastic moving vehicle loads, offering a comprehensive assessment of material property variability on structural response. For functionally graded material (FGM) beams, perturbation methods and point discretization techniques have been used to evaluate natural frequencies and mode shapes under stochastic material properties (Thuan & Hien, 2020). Other studies have applied MCs with spectral methods to investigate the vibrational characteristics of FGM beams with stochastic Young's modulus, contributing to improved structural designs in aerospace, mechanical, and civil engineering (Van Thuan & Chun, 2019).

Recent advancements in SFEM have significantly expanded its applications in structural analysis, particularly in composite and fiber-reinforced concrete structures. Mesoscale modeling techniques have been employed to investigate the mechanical response of fiber-reinforced concrete beams, allowing for a detailed examination of material randomness at the microscale and its influence on overall structural behavior (Al-Ahmed et al., 2022). Additionally, the integration of artificial intelligence (AI) with SFEM has emerged as a promising approach for enhancing predictive accuracy in composite laminate strength estimations. By leveraging machine learning algorithms and probabilistic modeling techniques, AI-enhanced SFEM can efficiently process large datasets and identify complex patterns in material behavior, leading to more accurate failure predictions and optimized design strategies (Nastos et al., 2023). In the domain of hybrid composite materials, numerical investigations have focused on the stochastic natural frequencies of such structures, emphasizing the essentiality of randomness characterization in dynamic response analysis. Thakkar & Karsh (2025) proposed a computational framework incorporating stochastic variations in material properties, demonstrating that random fluctuations in elastic modulus and other mechanical parameters significantly affect predicted natural frequencies and structural reliability. Furthermore, hybrid SFEM methodologies, such as integrating the Karhunen–Loève expansion with a modified perturbation-based SFEM, have been developed to enhance computational efficiency while preserving accuracy in large-scale structural analysis (Shao et al., 2023). These advancements highlight SFEM's potential in modern structural design, particularly when combined with high-performance computing and probabilistic modeling, to enhance the reliability of engineering systems.

These recent contributions underscore the necessity of incorporating refined SFEM techniques for a more comprehensive and systematic analysis of structures with three-dimensional (3D) spatially varying stochastic properties. As material uncertainties and external stochastic influences become increasingly significant in modern engineering applications, the development of robust SFEM methodologies will remain a crucial aspect of structural reliability assessment, ensuring that complex structural systems can withstand variable and unpredictable loading conditions while maintaining optimal performance and safety.

Recent advancements in stochastic structural analysis have introduced several innovative methodologies that enhance the accuracy and efficiency of uncertainty quantification. Higher-order stochastic techniques, notably Polynomial Chaos Expansion (PCE) and stochastic collocation, have gained prominence for their superior capability in capturing nonlinear structural behavior with reduced computational effort (Matthies & Keese, 2005; Xiu & Karniadakis, 2002). Simultaneously, the adoption of non-Gaussian and non-stationary random fields has been increasingly recognized for providing a more realistic characterization of material variability in practical engineering scenarios (Ghanem & Spanos, 2003; Kiureghian & Ke, 1988). Moreover, the integration of machine learning-based surrogate modeling has emerged as an effective strategy to mitigate the computational burden associated with large-scale stochastic simulations (Tripathy & Bilionis, 2018). Additionally, recent investigations have focused on the stochastic behavior of advanced materials, such as functionally graded materials and composites, under complex multi-dimensional random field conditions.

Despite numerous studies on the random response of beams due to stochastic material properties, most investigations primarily consider one-dimensional randomness. Limited research has addressed the effects of 3D randomness in material properties on beam responses. Real-world structures, particularly beams in bridge engineering, exhibit complex 3D spatial variability in properties such as Young's modulus. However, prior studies have not fully examined the influence of 3D stochastic variations on structural performance, nor have they developed an efficient and computationally feasible SFEM framework to address this issue. To address this gap, this study introduces an SFEM approach that employs the domain-weighted integration approach to represent the spatially varying 3D stochastic field of the elastic modulus, employing the perturbation-based method to investigate the stochastic static response of beams. To validate the accuracy of the developed SFEM, an independent MCs is conducted. Additionally, the study examines the sensitivity to correlation scales in the three-dimensional spatial domain and the variability of the 3D stochastic elastic modulus field on the coefficient of variation (COV) of displacement. Furthermore, by establishing a correlation between the COV of the random input (3D stochastic Young's modulus) and the random static response of the beam (COV of displacement), the study provides insights into the predictability of structural stochastic responses, which is critical for reliability assessment and engineering decision-making.

Bridges, in particular, are highly sensitive to material uncertainties, especially in aging infrastructure and deteriorated concrete structures. Understanding how 3D stochastic variability influences beam deflections is essential for improving reliability assessments, optimizing maintenance strategies, and enhancing safety evaluations in bridge engineering. In this context, the proposed SFEM serves as an efficient alternative to traditional MCs, facilitating large-scale stochastic analysis while significantly reducing computational costs. By enabling robust structural assessments under uncertainty, this methodology contributes to the advancement of probabilistic engineering design and risk-informed decision-making.

Given the significance of this research, this paper is organized to systematically present the development and application of SFEM for studying the static behavior of beams influenced by a 3D stochastic field of elastic parameters. To ensure a logical transition from theoretical formulation to numerical validation and result discussion, Section 2 introduces the weighted integration technique for discretizing the 3D stochastic spatial field of the material's elastic modulus and presents the formulation of SFEM combined with the perturbation approach. Section 3 describes the application of the proposed SFEM to analyze the stochastic static response of beams. Section 4 discusses the numerical results, focusing on the role of correlation distances and the variability measure of the three-dimensional spatial random distribution of the elastic property on the COV of displacement, with MCs employed as an independent validation method. Finally, Section 5 summarizes the key findings, investigates the reliability of the proposed SFEM method, and suggests potential directions for future research.

2. Discretization of the 3D Young's Modulus Stochastic Field using the Weighted Integration Method

For the convenience of readers in following the content of this study, **Table 1** in Appendix provides a comprehensive list of basic symbols along with their corresponding definitions used throughout the paper. Consider a simply supported beam with a rectangular cross-section, as illustrated in **Figure 1**. The Young's modulus of the beam is characterized by a spatially varying stochastic field in three dimensions, as defined in Equation (1).

$$E(x,y,z)=E_0\left[1+g_e(x,y,z)\right];\quad g_e(x,y,z)>-1 \tag{1}$$

The displacement field of the element is determined through the shape function (Logan, 2022) and nodal displacement vector of the element as:

$$u_i^e=[N]\{q\}_i^e \tag{2}$$

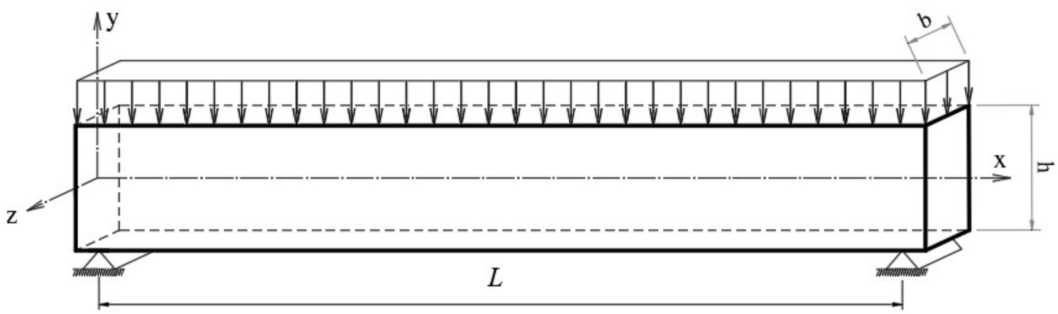

Figure 1. A beam model with stochastic material properties.

The element shape function matrix is determined as Equation (3), and the nodal displacement vector is determined as Equation (4).

$$[N]=[r][\Lambda] \tag{3}$$

$$\{q\}_i^e=\{q_1 \quad q_2 \quad q_3 \quad q_4\}^T \tag{4}$$

In which the matrix of constants $[\Lambda]$ depends on the length of the element defined as Equation (5). The matrix $[r]$ includes monomials defined as Equation (6).

$$[\Lambda]=\begin{bmatrix} 1 & 0 & 0 & 0 \\ 0 & 1 & 0 & 0 \\ -\frac{3}{L_e^2} & -\frac{2}{L_e} & \frac{3}{L_e^2} & -\frac{1}{L_e} \\ \frac{2}{L_e^3} & \frac{1}{L_e^3} & -\frac{2}{L_e^3} & \frac{1}{L_e^2} \end{bmatrix} \tag{5}$$

$$[r]=\left[x^0 \quad x^1 \quad x^2 \quad x^3\right] \tag{6}$$

In the context of the linear finite element method, the element stiffness matrix is written as follows:

$$[K]_e=\int_{V_e}[B]^T[D][B]dV_e \tag{7}$$

For beam elements, these matrices are determined as Equations (8) and (9).

$$[B]=-y[N"] \tag{8}$$

$$[D]=E(x,y,z) \tag{9}$$

By substituting Equations (8) and (9) into Equation (7) obtains Equation (10):

$$[K]_e=\int_{V_e}y^2[N"]^T E(x,y,z)[N"]dV_e \tag{10}$$

By substituting Equations (1), (5) and (6) into Equation (10) obtains Equation (11):

$$[K]_e = \underbrace{[\Lambda]^T \left\{ \int_{V_e} y^2 E_0 [r'']^T [r''] dV_e \right\} [\Lambda]}_{[K_0]_e} + \underbrace{[\Lambda]^T \left\{ \int_{V_e} y^2 g_e(x,y,z) E_0 [r'']^T [r''] dV_e \right\} [\Lambda]}_{[\Delta K]_e = \sum_{i=1}^{3} [\Delta K_i]_e} \tag{11}$$

with

$$[K_0]_e = \frac{E_0 I}{L_e^3} \begin{bmatrix} 12 & 6L_e & -12 & 6L_e \\ & 4L_e^2 & -6L_e & 2L_e^2 \\ & & 12 & -6L_e \\ sym & & & 4L_e^2 \end{bmatrix} \tag{12}$$

Based on Equation (6), $[r'']^T [r'']$ in Equation (11) is defined as Equation (13).

$$[r'']^T [r''] = \begin{bmatrix} 0 & 0 & 0 & 0 \\ 0 & 0 & 0 & 0 \\ 0 & 0 & 4 & 12x \\ 0 & 0 & 12x & 36x^2 \end{bmatrix} \tag{13}$$

The random variables are defined as:

$$\chi_i^e = \int_{V_e} x^{i-1} y^2 g_e(x,y,z) dV_e \quad ; \quad i = 1,2,3 \tag{14}$$

By substituting Equations (13) and (14) for $[\Delta K]_e$ in Equation (11) obtains Equation (15):

$$[\Delta K]_e = \underbrace{[\Lambda]^T \begin{bmatrix} 0 & 0 & 0 & 0 \\ 0 & 0 & 0 & 0 \\ 0 & 0 & 4 & 0 \\ 0 & 0 & 0 & 0 \end{bmatrix} [\Lambda]}_{[\Delta K_1]_e} \chi_1^e + \underbrace{[\Lambda]^T \begin{bmatrix} 0 & 0 & 0 & 0 \\ 0 & 0 & 0 & 0 \\ 0 & 0 & 0 & 12 \\ 0 & 0 & 12 & 0 \end{bmatrix} [\Lambda]}_{[\Delta K_2]_e} \chi_2^e + \underbrace{[\Lambda]^T \begin{bmatrix} 0 & 0 & 0 & 0 \\ 0 & 0 & 0 & 0 \\ 0 & 0 & 0 & 0 \\ 0 & 0 & 0 & 36 \end{bmatrix} [\Lambda]}_{[\Delta K_3]_e} \chi_3^e \tag{15}$$

The matrices appearing in Equation (15) are defined as Equation (16), (17), and (18).

$$[\Delta K_1]_e = \frac{E_0}{L_e^6} \begin{bmatrix} 36L_e^2 & 24L_e^3 & -36L_e^2 & 12L_e^3 \\ & 16L_e^4 & -24L_e^3 & 8L_e^4 \\ & & 36L_e^2 & -12L_e^3 \\ sym & & & 4L_e^4 \end{bmatrix} \tag{16}$$

$$[\Delta K_2]_e = \frac{E_0}{L_e^6} \begin{bmatrix} -144L_e & -84L_e^2 & 144L_e & -60L_e^2 \\ & -48L_e^3 & 84L_e^2 & -36L_e^3 \\ & & -144L_e & 60L_e^2 \\ sym & & & -24L_e^3 \end{bmatrix} \tag{17}$$

$$\left[\Delta K_3\right]_e = \frac{E_0}{L_e^6}\begin{bmatrix} 144 & 72L_e & -144 & 72L_e \\ & 36L_e^2 & -72L_e & 36L_e^2 \\ & & 144 & -72L_e \\ sym & & & 36L_e^2 \end{bmatrix} \tag{18}$$

Random variables defined as Equation (14) are called basic stochastic quantities. Due to the fact that these random variables are discretized from the same stochastic field, these random variables are correlated with each other.

3. Random Static Response Analysis of Beams with 3D Stochastic Elastic Modulus using SFEM

In the context of the standard FEM of linear analysis of static problems. The equilibrium equation obtained after discretizing the structural geometry usually takes the form like Equation (19).

$$\left[K\right]\left\{U\right\} = \left\{P\right\} \tag{19}$$

$[K]$ is determined based on the stiffness matrix of the elements, as in Equation (20):

$$\left[K\right] = \sum_{e=1}^{N_e}\left[K\right]_e \tag{20}$$

By substituting Equations (11) and (15) into Equation (20) obtains Equation (21):

$$\left[K\right] = \sum_{e=1}^{N_e}\left[K_0\right]_e + \sum_{e=1}^{N_e}\left\{\left[\Delta K_1\right]_e \chi_1^e + \left[\Delta K_2\right]_e \chi_2^e + \left[\Delta K_3\right]_e \chi_3^e\right\} \tag{21}$$

In this study the load considered is determined. Young's modulus is assumed to be a 3D Gaussian univariate stationary stochastic field with zero expectation. Young's modulus varies around the mean value E_0. Therefore, the nodal displacement vector and the global stiffness matrix also vary around the values $\left\{U_0\right\}$, K_0. The stiffness matrix K_0 is determined based on E_0 as Equation (22).

$$K_0 = \sum_{e=1}^{N_e}\left[K_0\right]_e \tag{22}$$

$[K]$ depends linearly on the random variables. The random field of Young's modulus is discretized into a set of random variables $\left\{\chi\right\} = \left\{\chi_i^e\right\}_{i=1,2,3}^{e=1,2,\ldots,N_e}$. The elastic modulus random field is a Gaussian random field with a mean of zero, then the random variables are also Gaussian random variables and have zero mean. Therefore, Equation (19) can be rewritten as Equation (23) as follows:

$$\left[K\left(\left\{\chi\right\}\right)\right]\left\{U\left(\left\{\chi\right\}\right)\right\} = \left\{P\right\} \tag{23}$$

The overall stiffness matrix and the nodal displacement vector in Equation (20) are expanded according to the Taylor series around its mean value as follows:

$$\left[K\left(\left\{\chi\right\}\right)\right] \approx K_0 + \sum_{e=1}^{N_e}\sum_{i=1}^{3}\left[K_i^e\right]_I \chi_i^e + \frac{1}{2}\sum_{e_1=1}^{N_e}\sum_{e_2=1}^{N_e}\sum_{i_1=1}^{3}\sum_{i_2=1}^{3}\left[K_{i_1 i_2}^{e_1 e_2}\right]_{II} \chi_{i_1}^{e_1}\chi_{i_2}^{e_2} + \ldots \tag{24}$$

$$\left\{U\left(\{\chi\}\right)\right\} \approx \{U_0\} + \sum_{e=1}^{N_e}\sum_{i=1}^{3}\left\{U_i^e\right\}_I \chi_i^e + \frac{1}{2}\sum_{e_1=1}^{N_e}\sum_{e_2=1}^{N_e}\sum_{i_1=1}^{3}\sum_{i_2=1}^{3}\left\{U_{i_1 i_2}^{e_1 e_2}\right\}_{II} \chi_{i_1}^{e_1}\chi_{i_2}^{e_2} + \ldots \tag{25}$$

$\left[K_i^e\right]_I$ and $\left[K_{i_1 i_2}^{e_1 e_2}\right]_{II}$ represent the first and second partial derivatives of the global stiffness matrix, evaluated $\{\chi\}=0$. They are defined as follows:

$$\left[K_i^e\right]_I = \left.\frac{\partial K}{\partial \chi_i^e}\right|_{\{\chi\}=0} \tag{26}$$

$$\left[K_{i_1 i_2}^{e_1 e_2}\right]_{II} = \left.\frac{\partial^2 K}{\partial \chi_{i_1}^{e_1}\partial \chi_{i_2}^{e_2}}\right|_{\{\chi\}=0} \tag{27}$$

Similarly, $\left\{U_i^e\right\}_I$ and $\left\{U_{i_1 i_2}^{e_1 e_2}\right\}_{II}$ are the first partial derivatives and the second partial derivative of $\{U\}$ at $\{\chi\}=0$ as Equations (28) and (29).

$$\left\{U_i^e\right\}_I = \left.\frac{\partial U}{\partial \chi_i^e}\right|_{\{\chi\}=0} \tag{28}$$

$$\left\{U_{i_1 i_2}^{e_1 e_2}\right\}_{II} = \left.\frac{\partial^2 U}{\partial \chi_{i_1}^{e_1}\partial \chi_{i_2}^{e_2}}\right|_{\{\chi\}=0} \tag{29}$$

Substituting Equations (24) and (25) into Equation (23) determines the coefficients of the same order on both sides of Equation (23) to obtain the following equations:

The zero-order:

$$\{U_0\} = K_0^{-1}\{P\} \tag{30}$$

The first-order:

$$\left\{U_i^e\right\}_I = -K_0^{-1}\left[K_i^e\right]_I \{U_0\} \tag{31}$$

The second-order:

$$\left\{U_{i_1 i_2}^{e_1 e_2}\right\}_{II} = K_0^{-1}\left\{-\left[K_{i_1}^{e_1}\right]_I\left\{U_{i_2}^{e_2}\right\}_I - \left[K_{i_2}^{e_2}\right]_I\left\{U_{i_1}^{e_1}\right\} - \left[K_{i_1 i_2}^{e_1 e_2}\right]_{II}\{U_0\}\right\} \tag{32}$$

Substituting Equation (31) into Equation (25) gives a first-order approximation of $\{U\}$ vector determined as Equation (33):

$$\{U\} \approx \{U_0\} - \sum_{e=1}^{N_e}\sum_{i=1}^{3} K_0^{-1}\left[K_i^e\right]_I \{U_0\}\chi_i^e \tag{33}$$

Calculating the expectation and variance of the nodal displacement vector $\{U\}$ through the approximation series presented in Equation (33) yields the following results.

$$\mu\left[\{U\}\right] \approx \{U_0\} \tag{34}$$

$$Cov\left[\{U\},\{U\}\right] = \sum_{e_1=1}^{N_e}\sum_{i_1=1}^{3}\sum_{e_2=1}^{N_e}\sum_{i_2=1}^{3} K_0^{-1}\left[K_{i_1}^{e_1}\right]_I \{U_0\}\{U_0\}^T \left(\left[K_{i_2}^{e_2}\right]_I\right)^T \left(K_0^{-1}\right)^T \mu\left[\chi_{i_1}^{e_1}\chi_{i_2}^{e_2}\right] \tag{35}$$

Because the stiffness matrix of an element is a first-order function of the underlying random variables, the global stiffness matrix [*K*] determined from the element stiffness matrix in the context of the FEM is also a function linearity of the basic random. The first partial derivative of [*K*] is determined as Equation (36). $\left[\Delta K_i\right]_{e,E}$ is a random part of the $\left[K\right]_e$ expanded according to the size of the global stiffness matrix.

$$\left[K_i^e\right]_I = \left[\Delta K_i\right]_{e,E} \tag{36}$$

Substituting Equation (36) into Equation (35) the covariance matrix of the displacement vector is defined as:

$$Cov\left[\{U\},\{U\}\right] = \sum_{e_1=1}^{N_e}\sum_{i_1=1}^{3}\sum_{e_2=1}^{N_e}\sum_{i_2=1}^{3} K_0^{-1}\left[\Delta K_{i_1}\right]_{e_1,E} \{U_0\}\{U_0\}^T \left[\Delta K_{i_2}\right]_{e_2,E}^T \left(K_0^{-1}\right)^T \mu\left[\chi_{i_1}^{e_1}\chi_{i_2}^{e_2}\right] \tag{37}$$

Pay attention to Equation (14); the expected value in Equation (37) is defined as Equation (38):

$$\mu\left[\chi_{i_1}^{e_1}\chi_{i_2}^{e_2}\right] = \int_{V_{e_2}}\int_{V_{e_2}} x_1^{i_1-1}y_1^{2}x_2^{i_2-1}y_2^{2}\mu\left[g_{e_1}(x_1,y_1,z_1)\,g_{e_2}(x_2,y_2,z_2)\right]dV_{e_1}dV_{e_2} \tag{38}$$

The expected value in integral (38) is determined through the autocorrelation function of the random field.

$$\mu\left[g_{e_1}(x_1,y_1,z_1)\,g_{e_2}(x_2,y_2,z_2)\right] = R_{gg} \tag{39}$$

Substituting Equation (39) into Equations (38) and (38) into Equation (37), Equation (37) can be rewritten as follows:

$$Cov\left[\{U\},\{U\}\right] = \sum_{e_1=1}^{N_{e_1}}\sum_{i_1=1}^{3}\sum_{e_2=1}^{N_{e_2}}\sum_{i_2=1}^{3} \left\{\begin{matrix} K_0^{-1}\left[\Delta K_{i_1}\right]_{e_1,E}\{U_0\} \\ \{U_0\}^T\left[\Delta K_{i_2}\right]_{e_2,E}^T\left(K_0^{-1}\right)^T \end{matrix}\right\} \int_{V_{e_2}}\int_{V_{e_2}} x_1^{i_1-1}y_1^{2}x_2^{i_2-1}y_2^{2}R_{gg}\,dV_{e_1}dV_{e_2} \tag{40}$$

The variance vector of $\{U\}$ includes terms located on the main diagonal of the covariance matrix of the nodal displacement vector defined as Equation (41):

$$Var\left[\{U\},\{U\}\right] = \sum_{e_1=1}^{N_e}\sum_{i_1=1}^{3}\sum_{e_2=1}^{N_e}\sum_{i_2=1}^{3} diag\left\{\begin{matrix} K_0^{-1}\left[\Delta K_{i_1}\right]_{e_1,E}\{U_0\} \\ \{U_0\}^T\left[\Delta K_{i_2}\right]_{e_2,E}^T\left(K_0^{-1}\right)^T \end{matrix}\right\} \int_{V_{e_2}}\int_{V_{e_2}} x_1^{i_1-1}y_1^{2}x_2^{i_2-1}y_2^{2}R_{gg}\,dV_{e_1}dV_{e_2} \tag{41}$$

Equation (42) defines the COV of displacement at the mid-span of the beam as the ratio of the displacement fluctuation at mid-span to the absolute value of the expected displacement.

$$\mathrm{COV} = \frac{\sqrt{Var\left[\{U\},\{U\}\right]_{\frac{L}{2}}}}{\mu\left[\{U\}\right]_{\frac{L}{2}}} \tag{42}$$

4. Results and Discussion

In this study, we develop an independent Monte Carlo simulation (MCs) using the spectral representation method to generate random samples (Shinozuka & Deodatis, 1991, 1996), combined with deterministic FEM, to assess the random static performance of beams. The results include the displacement variation of a beam with a 3D uncertain modulus of the material's elasticity. The COV of displacement from MCs is compared with that obtained from SFEM. MCs techniques have been widely applied in stochastic structural analysis (Papadrakakis & Kotsopulos, 1999; Schuëller, 2001). In practice, MCs involves: (1) identifying random input data; (2) generating random samples based on probability distributions; (3) performing deterministic analyses for each sample; and (4) using statistical tools to determine the structural response characteristics.

The spectral representation method is employed to generate numerical sample functions for the Gaussian, three-dimensional, univariate, zero-mean, and homogeneous random field of the elastic property parameter. For a 3D stochastic field, the random field can be represented as Equation (43).

$$g(x,y,z)=\sqrt{2}\sum_{n_1=0}^{N_1-1}\sum_{n_2=0}^{N_2-1}\sum_{n_3=0}^{N_3-1}\left\{\begin{array}{l} A^{(1)}_{n_1n_2n_3}\cos\left[\kappa_{1n_1}x+\kappa_{2n_2}y+\kappa_{3n_3}z+\Phi^{(1)}_{n_1n_2n_3}\right] \\ +A^{(2)}_{n_1n_2n_3}\cos\left[\kappa_{1n_1}x+\kappa_{2n_2}y-\kappa_{3n_3}z+\Phi^{(2)}_{n_1n_2n_3}\right] \\ +A^{(3)}_{n_1n_2n_3}\cos\left[\kappa_{1n_1}x-\kappa_{2n_2}y+\kappa_{3n_3}z+\Phi^{(3)}_{n_1n_2n_3}\right] \\ +A^{(4)}_{n_1n_2n_3}\cos\left[\kappa_{1n_1}x-\kappa_{2n_2}y-\kappa_{3n_3}z+\Phi^{(4)}_{n_1n_2n_3}\right] \end{array}\right\} \tag{43}$$

with

$$A^{(i)}_{0n_2n_3}=A^{(i)}_{n_10n_3}=A^{(i)}_{n_1n_20}=0 \quad ; \; i=1,2,3,4 \tag{44}$$

In Equation (43) the coefficients $A^{(i)}_{n_1n_2n_3}$ are determined as follows:

$$A^{(1)}_{n_1n_2n_3}=\sqrt{2S_{gg}\left(\kappa_{1n_1},\kappa_{2n_2},\kappa_{3n_3}\right)\Delta\kappa_1\Delta\kappa_2\Delta\kappa_3} \tag{45}$$

$$A^{(2)}_{n_1n_2n_3}=\sqrt{2S_{gg}\left(\kappa_{1n_1},\kappa_{2n_2},-\kappa_{3n_3}\right)\Delta\kappa_1\Delta\kappa_2\Delta\kappa_3} \tag{46}$$

$$A^{(3)}_{n_1n_2n_3}=\sqrt{2S_{gg}\left(\kappa_{1n_1},-\kappa_{2n_2},\kappa_{3n_3}\right)\Delta\kappa_1\Delta\kappa_2\Delta\kappa_3} \tag{47}$$

$$A^{(4)}_{n_1n_2n_3}=\sqrt{2S_{gg}\left(\kappa_{1n_1},-\kappa_{2n_2},-\kappa_{3n_3}\right)\Delta\kappa_1\Delta\kappa_2\Delta\kappa_3} \tag{48}$$

κ_{in_i} in Equations (45) - (48) is determined as Equations (49) - (51):

$$\kappa_{1n_1}=n_1\Delta\kappa_1 \qquad n_1=1,2,...,N_1-1 \tag{49}$$

$$\kappa_{2n_2}=n_2\Delta\kappa_2 \qquad n_2=1,2,...,N_2-1 \tag{50}$$

$$\kappa_{3n_3}=n_3\Delta\kappa_3 \qquad n_3=1,2,...,N_3-1 \tag{51}$$

$\Delta\kappa_i$ in Equations (45) - (48) is determined as Equation (52):

$$\Delta\kappa_1=\frac{\kappa_{1u}}{N_1} \quad ; \quad \Delta\kappa_2=\frac{\kappa_{2u}}{N_2} \quad ; \quad \Delta\kappa_3=\frac{\kappa_{3u}}{N_3} \tag{52}$$

The power spectral density of the stationary, zero-mean, univariate Gaussian random field in three dimensions used in Equations (45) - (48) is written as:

$$S_{gg}\left(\kappa_1,\kappa_2,\kappa_3\right)=\sigma_g^2\frac{d_x d_y d_z}{4\pi}\exp\left[-\left(\frac{d_x\kappa_1}{2}\right)^2-\left(\frac{d_y\kappa_2}{2}\right)^2-\left(\frac{d_z\kappa_3}{2}\right)^2\right] \tag{53}$$

κ_{iu} in Equation (52) denotes the upper cut-off wave numbers. κ_{iu} is determined as expressed in Equation (54), with ξ representing the error.

$$\int_0^{\kappa_{1u}}\int_{-\kappa_{2u}}^{\kappa_{2u}}\int_{-\kappa_{3u}}^{\kappa_{3u}} S_{gg}\left(\kappa_1,\kappa_2,\kappa_3\right)d\kappa_1 d\kappa_2 d\kappa_3=\left(1-\xi\right)\int_0^{\infty}\int_{-\infty}^{\infty}\int_{-\infty}^{\infty} S_{gg}\left(\kappa_1,\kappa_2,\kappa_3\right)d\kappa_1 d\kappa_2 d\kappa_3 \tag{54}$$

Figure 2 presents a sample realization of the beam’s elastic modulus with random variation across three spatial dimensions, displayed using the spectral representation method at cross-sections of $x = 0$, $x = L/4$, $x = L/2$, and $x = L$.

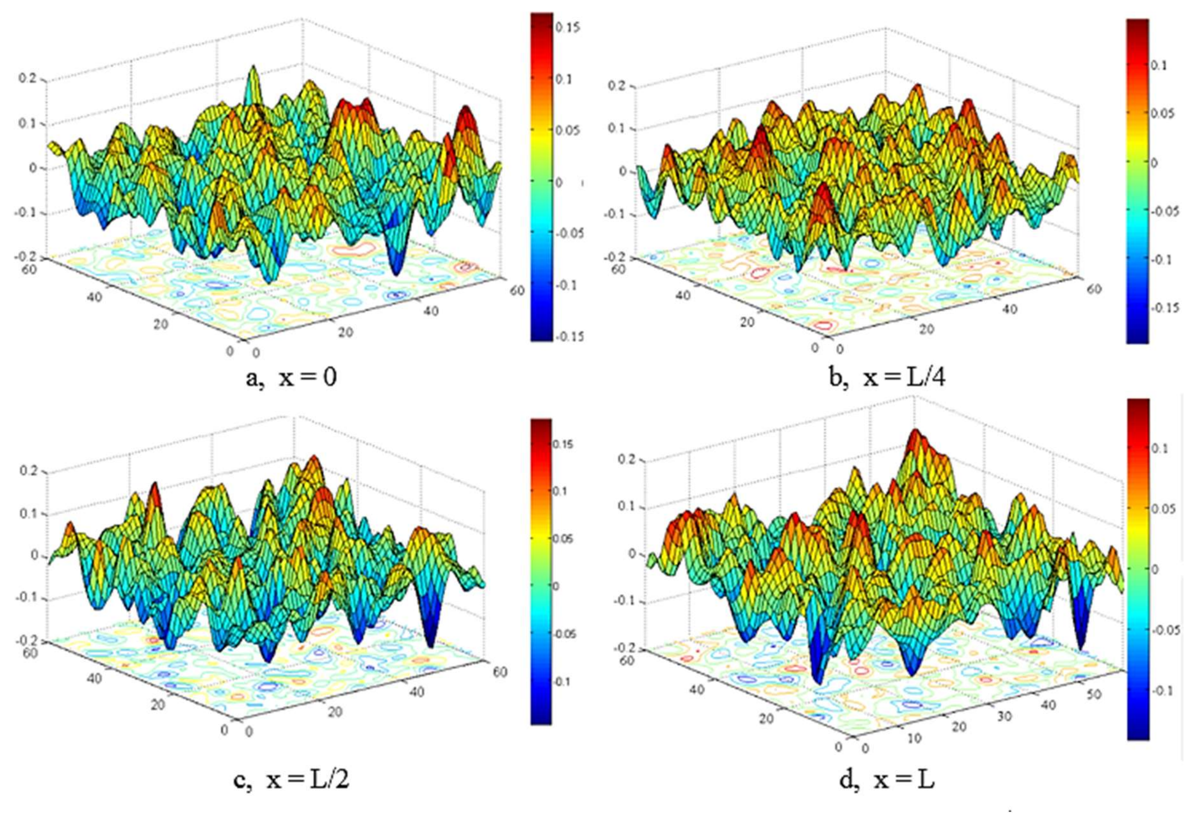

Figure 2. The realization of the 3D random field of Young’s modulus.

Consider a simple beam with a rectangular cross-section subjected to a uniformly distributed load q = 10 kN/m. The beam has geometric dimensions including: Span length L = 6 m, cross-sectional height h = 0.6 m, cross-sectional width b = 0.3 m. Young's modulus is considered a zero-mean, stationary, univariate, 3D

Gaussian stochastic field with $E_0 = 30\times10^3$ MPa. The self-correlation function associated with the stochastic field of the elastic modulus is assumed to be as given in Equation (55).

$$R_{gg}\left(\xi_1,\xi_2,\xi_3\right)=\sigma_g^2\exp\left[-\left(\frac{\xi_1}{d_x}\right)^2-\left(\frac{\xi_2}{d_y}\right)^2-\left(\frac{\xi_3}{d_z}\right)^2\right] \tag{55}$$

where, $\xi_1 = x_2 - x_1$, $\xi_2 = y_2 - y_1$, and $\xi_3 = z_2 - z_1$ are the separation distances along the x, y and z directions respectively.

This study verifies the accuracy of the SFEM, formulated to analyze the static response of a beam with a 3D random modulus of elasticity, by comparing the COV of the mid-span displacement with the COV derived from MCs statistical analysis. Specifically, 10,000 realizations of the 3D random Young's modulus field are generated using the Equation (43), and deterministic FEM is performed on each realization to obtain the corresponding deflections. The resulting sample of deflections is then statistically analyzed to produce frequency distributions, as shown in **Figure 3**, for several correlation lengths defined as $d_x = d_y = d_z = d$, with d taking values of 0.05L, 0.1L, L, and 15L, and with $\sigma_g = 0.05$.

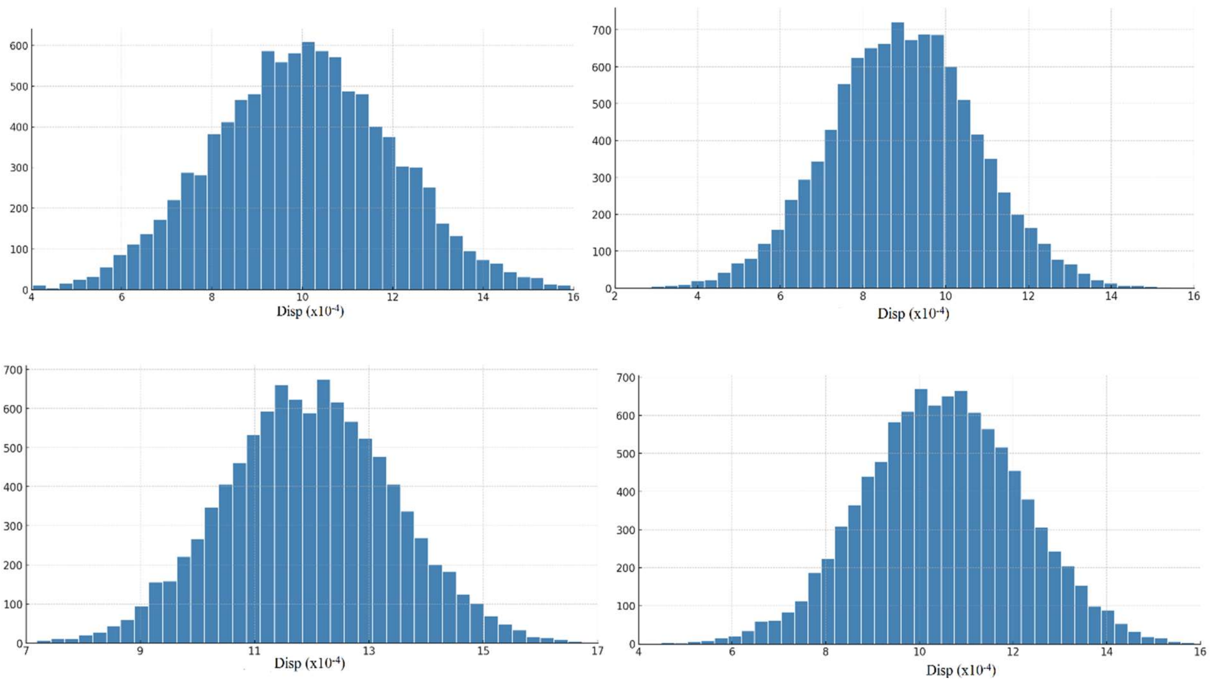

Figure 3. Frequency histogram of displacement at the mid-span of the beam ($\sigma_g = 0.05$).

Statistical processing of the displacement dataset obtained from MCs facilitates the determination of key statistical characteristics, including the mean, variance, standard deviation, and COV of displacement. These parameters play a crucial role in evaluating the variability of structural responses due to the influence of the stochastic Young's modulus field. **Figure 4** presents a comparison of the COV of mid-span displacement determined using SFEM and MCs. The correlation distance in space, defined as $d_x = d_y = d_z = d$, oscillates between 0.001L and 100L, corresponding to the case $\sigma_g = 0.05$. The analysis of COV values obtained through the two methods reveals relatively minor differences when assessed at small spatial correlation lengths of the stochastic field. Conversely, a substantial increase in correlation length leads to a progressive reduction in the COV disparity between the two methods. The SFEM and MCs outputs exhibit a trend of convergence toward near-identity at large correlation lengths. This confirms that SFEM achieves high accuracy and can effectively replace MCs. This is particularly advantageous in large-scale models, where reducing computational cost is a critical factor. Indeed, the proposed SFEM formulation in this study establishes governing equations for statistical quantities through an approximation series, thereby significantly reducing computational cost while maintaining accuracy. Furthermore, the strong agreement between SFEM and MCs outcomes at large correlation lengths suggests that when the stochastic field exhibits strong spatial correlation, the local material fluctuations diminish, leading to a more homogeneous structural response. This observation implies that the influence of stochasticity in the elastic modulus decreases as the correlation length increases, reinforcing the validity and efficiency of SFEM in stochastic structural mechanics problems characterized by high uncertainty.

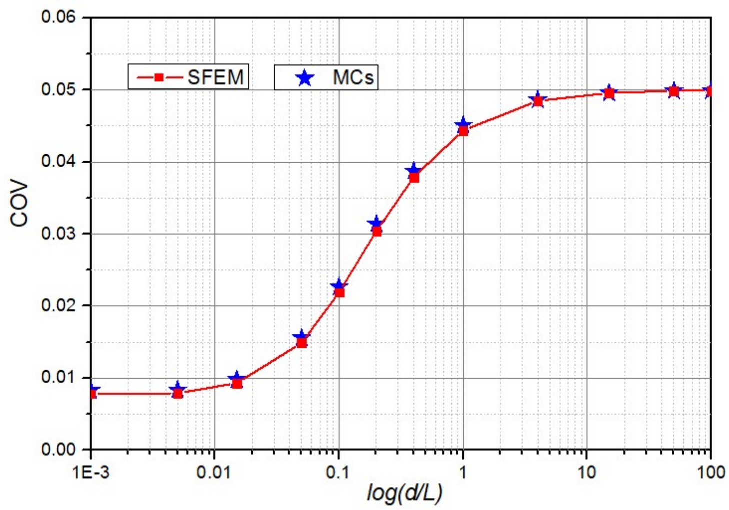

Figure 4. Evaluation of COV using SFEM and MCs in comparison ($\sigma_g = 0.05$).

This work analyzes how the correlation lengths affect the COV of displacement. Three correlation length cases are considered: d_x=*d*, d_y=d_z=*d*; d_y=*d*, d_x=d_z=*d*; d_z=*d*, d_x=d_y=*d*, where *d* takes values from 0.001L up to 100L and $\sigma_g = 0.05$. The results, illustrated in **Figure 5**, reveal similar trends of the COV of displacement for all cases. Specifically, the COV increases with increasing correlation length, with a more pronounced increase observed for smaller correlation lengths. For instance, in the case of d_x=*d*, d_y=d_z=*d*, doubling the correlation length from 0.1L to 0.2L results in a 1.388-fold increase in the COV, from 0.0219 to 0.0304. Conversely, doubling the correlation length from *50*L to *100*L yields a negligible increase in the COV, approximately 1.002 times, from 0.0498 to 0.0499. Notably, the COV of deflection asymptotically stabilizes at the statistical deviation of the stochastic Young's modulus field as the correlation lengths increase indefinitely. Furthermore, the influence of correlation length along the beam's longitudinal direction on the COV of displacement is significantly greater than that of the correlation lengths along the other axes. This can be explained by the fact that the beam's length is the primary load-bearing direction, meaning that the spatial distribution of the stochastic Young's modulus in this direction directly affects the overall stiffness of the structure. As the correlation length along the beam's longitudinal axis increases, the stochastic variations in the Young's modulus become more uniform over the entire length, thereby reducing localized randomness effects and leading to greater stability in displacement responses. In contrast, increasing the correlation length along the other axes has a relatively smaller impact on the beam's overall stiffness, as these directions are primarily associated with shear stiffness or higher-order deformation modes.

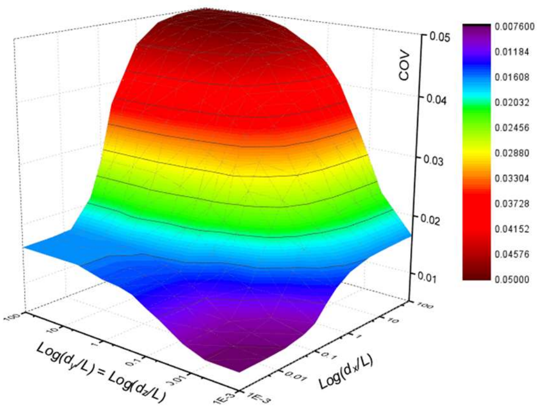

a, d_x=d, d_y=d_z=d

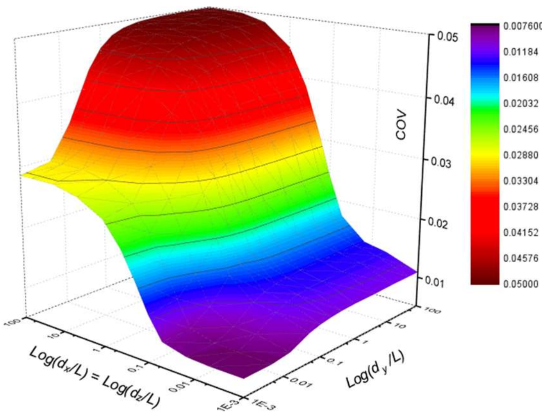

b, d_y=d, d_x=d_z=d

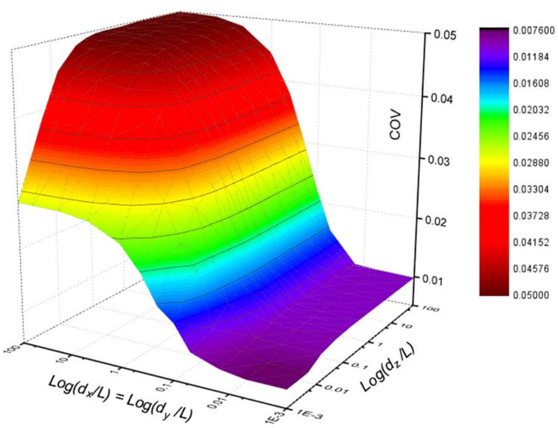

c, *d_z=d, d_x=d_y=d*

Figure 5. The impact of correlation lengths in the 3D directions of space on the COV.

Figure 6 details the analysis of how correlation distances affect the displacement COV in the Young's modulus modeled as a 3D stochastic field, across different σ_g values. The correlation distances investigated in this case is $d_x = d_y = d_z = d$, in which d takes values fluctuating between 0.001L and 100L, associated with four different values of σ_g: 0.05, 0.10, 0.15, and 0.20. The COV of displacement exhibits a positive correlation with σ_g at all investigated correlation distances. The increased dispersion of the elastic modulus around its mean value leads to a wider dispersion of displacement around its mean value, resulting in an increase in the COV of displacement as σ_g increases.

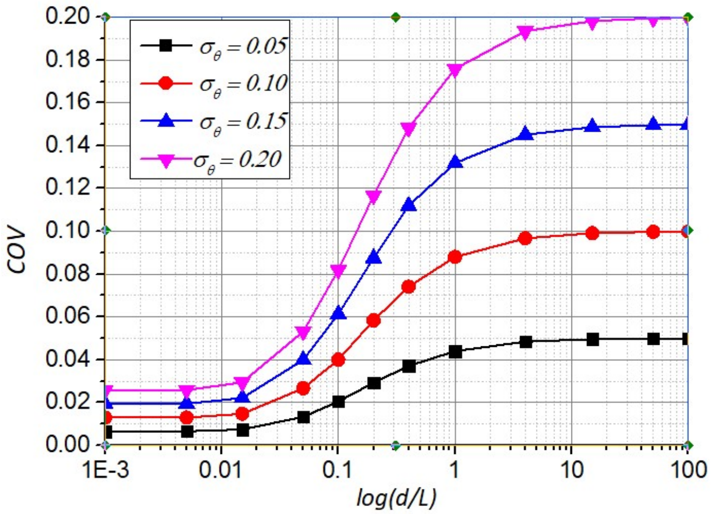

Figure 6. Relationship between COV and correlation lengths corresponding to different values of σ_g.

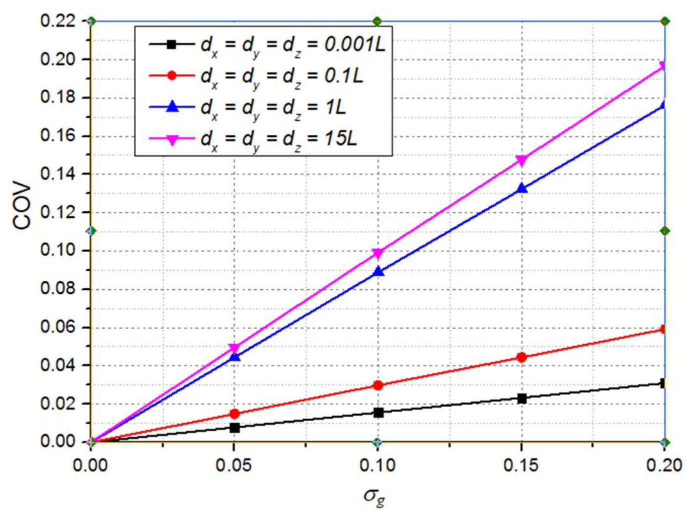

Figure 7. Relationship between COV of displacement and σ_g.

The 3D randomness of the elastic modulus is mathematically described as a 3D stochastic field with zero mean. Consequently, the COV of Young's modulus is equal to the standard deviation of the 3D random field. Therefore, the correlation between the COV of displacement and σ_g is equivalent to the correlation between the COV of displacement and the COV of Young's modulus. This relationship is illustrated in **Figure 7** with several correlation distances taken into account, namely: d_x=d_y=d_z=d, with d assigned values of 0.001L, 0.1L, 1L, and 100L. The findings derived from the analysis imply that there is a linear-like trend between the COV of displacement and σ_g; or in other words, between the COV of displacement as the static random response of the beam and the COV of the elastic modulus as the random input. Thanks to this near-linear relationship, it is possible to predict the static random response of the structure when the statistical properties of the stochastic input, specifically the elastic modulus, are known.

The uncertainty-driven response of the beam was evaluated using statistical analysis techniques, with the COV of displacement computed to quantify variability. MCs were conducted to establish a benchmark dataset for validating the SFEM, with convergence assessed based on the stabilization of statistical moments. The spectral representation method was employed to generate numerical sample functions of the three-dimensional Gaussian random field, ensuring consistency in the stochastic field representation. Despite the robustness of the proposed methodology, several limitations must be acknowledged. The first-order perturbation approach used in SFEM may introduce approximation errors in cases involving strong material nonlinearity, highlighting the need for higher-order stochastic approximations in future research. Additionally, the assumption of a Gaussian homogeneous random field for Young's modulus may not fully capture real-world material variations, necessitating further exploration of non-Gaussian and non-stationary random fields. Furthermore, while MCs serve as an independent validation method, their computational cost remains a significant challenge for large-scale structural models, suggesting the potential benefits of advanced variance reduction techniques or surrogate modeling approaches.

5. Conclusions

This study presents a comprehensive stochastic finite element framework for analyzing the static response of beams with spatially varying Young's modulus modeled as a three-dimensional (3D) random field. By integrating the weighted integration method for random field discretization with a perturbation-based SFEM approach, the proposed methodology effectively captures the influence of stochastic material variations in all three spatial dimensions. The accuracy of the developed SFEM is rigorously validated through MCs, demonstrating strong agreement between the two approaches, with only negligible discrepancies observed, particularly for large correlation distances. The results indicate that the coefficient of variation (COV) of mid-span deflections exhibits an increasing trend as the correlation length of the stochastic field grows. It is of particular significance that, in the asymptotic limit of infinite correlation length, the COV of deflections exhibits an asymptotic equivalence to the standard deviation of the stochastic three-dimensional Young's modulus field. Furthermore, this study establishes a strong positive correlation between the COV of deflections and the standard deviation of the random Young's modulus field, revealing that greater dispersion in material properties leads to increased variability in structural response. A key finding is the nearly linear relationship between the COV of beam displacement and the COV of Young's modulus, providing critical insights into the predictability of stochastic structural behavior.

This research contributes significantly to the body of knowledge in stochastic structural analysis by advancing the application of SFEM to 3D random fields, an area that has received limited attention in prior studies. While most existing research primarily considers one-dimensional randomness in material properties, this study extends the stochastic modeling framework to account for spatially correlated uncertainties in all three dimensions. The findings enhance the understanding of 3D stochastic effects on beam behavior and provide a robust foundation for future investigations into more complex structural systems under uncertainty.

The developed stochastic finite element framework offers a practical approach for analyzing the structural behavior of beams with spatially varying material properties. This method can be applied to the reliability assessment and performance optimization of advanced structures in aerospace, civil, and mechanical engineering, where material uncertainties are unavoidable. By incorporating spatial randomness into the analysis, the proposed method enhances the accuracy of structural predictions and supports informed decision-making in engineering design.

Despite the advances presented in this work, several directions remain open for future research. Extending the proposed SFEM framework to nonlinear and dynamic problems, such as large-deformation analysis, material nonlinearity, and time-dependent stochastic loading, would enhance its applicability. Additionally, exploring higher-order stochastic approximations, including polynomial chaos expansion (PCE) and stochastic collocation methods, could improve accuracy, particularly in cases where material property fluctuations are significant. Future studies may also investigate the impact of non-Gaussian and non-stationary random fields to achieve a more realistic representation of material uncertainties in practical applications. Moreover, applying the developed methodology to more complex structural systems, such as functionally graded materials (FGMs), laminated composites, and multi-material assemblies, would broaden its practical significance. Further improvements in computational efficiency could be achieved through advanced variance reduction techniques, surrogate modeling, and parallel computing. Finally, experimental validation through physical testing of materials with spatially varying properties would provide valuable insights into the accuracy and reliability of the proposed stochastic analysis framework.

Conflict of Interest

The authors confirm that there is no conflict of interest to declare for this publication.

Acknowledgments

This research is funded by the Ministry of Education and Training (MOET), Vietnam under the grant number B2023-GHA-09.

AI Disclosure

During the preparation of this work the author(s) used generative AI in order to improve the language of the article. After using this tool/service, the author(s) reviewed and edited the content as needed and take(s) full responsibility for the content of the publication.

Appendix

Table 1. Explanation of the symbols in the paper.

Symbol	Description	Symbol	Description
L	Span length of the beam structure	χ_i^e	Elemental basic random variable
h	Height of the rectangular beam cross-section	$\{\chi\}$	Global basic random variables of the structure
b	Width of the rectangular beam cross-section	$[K]$	Structural stiffness matrix of the beam
$E(x,y,z)$	3D stochastic Young's modulus of the beam	$\{U\}$	Global nodal displacement vector of the beam structure
E_0	Expectation of Young's modulus	$\{P\}$	Global nodal load vector of the beam structure
$g_e(x,y,z)$	Stationary, univariate 3D stochastic field	$\{U_0\}$	Deterministic part of the global nodal displacement vector
u_i^e	Elemental beam displacement	$[K_0]$	Deterministic part of the global stiffness matrix
$[N]$	Shape function matrix of the beam element	$Cov[.]$	Covariance
$\{q\}_i^e$	Displacement vector at beam element nodes	$\mu[.]$	Mean value
L_e	Elemental beam length	R_{gg}	Autocorrelation function
$[K]_e$	Stiffness matrix of the beam element	S_{gg}	Power spectral density function
$[B]$	Strain-displacement matrix	Var	Standard deviation
[D]	Elasticity matrix	COV	Coefficient of variation
$[N'']$	Second-order derivative matrix of the shape function	$A_{n_1n_2n_3}^{(i)}$	Amplitude of the stochastic function series
y	Distance between the neutral axis and the point under consideration	$\Phi_{n_1n_2n_3}^{(i)}$	Initial phase of the stochastic function series
$[K_0]_e$	Deterministic part of the elemental stiffness matrix	κ_{in_i}	Cut-off angular frequency
N_e	Number of elements	N_i	Number of stochastic functions
$[\Delta K_i]_e$	Stochastic part of the elemental stiffness matrix	d_x,d_y,d_z	Correlation lengths along the axes
I	Cross-sectional moment of inertia of the beam	σ_g	Standard deviation of the stochastic field

References

Adhikari, S., & Mukherjee, S. (2022). The exact element stiffness matrices of stochastically parametered beams. *Probabilistic Engineering Mechanics*, *69*, 103317. https://doi.org/10.1016/j.probengmech.2022.103317.

Al-Ahmed, H.A.A., Al-Rumaithi, A., Allawi, A.A., & El-Zohairy, A. (2022). Mesoscale analysis of fiber-reinforced concrete beams. *Engineering Structures*, *266*, 114575. https://doi.org/10.1016/j.engstruct.2022.114575.

Arregui-Mena, J.D., Margetts, L., & Mummery, P.M. (2016). Practical application of the stochastic finite element method. *Archives of Computational Methods in Engineering*, *23*(1), 171-190. https://doi.org/10.1007/s11831-014-9139-3.

Cao, X., Qi, Y., Li, E., Huang, J., Yan, A., & Xu, D. (2024). Analyzing uncertainties in multilayer steel frame structures: A reliability test using the stochastic finite element method. *Materials Express*, *14*(2), 230-242. https://doi.org/10.1166/mex.2024.2617.

Chakraborty, S., & Bhattacharyya, B. (2002). An efficient 3D stochastic finite element method. *International Journal of Solids and Structures*, *39*(9), 2465-2475. https://doi.org/10.1016/S0020-7683(02)00080-X.

Danh, L.B. (2024). Research on numerical models to simulate the blast loads on reinforced concrete structures using abaqus software. *Transport and Communications Science Journal*, *75*(3), 1452-1462. https://doi.org/10.47869/tcsj.75.3.11.

Deodatis, G. (1990). Bounds on response variability of stochastic finite element systems. *116*(3), 565-585. https://doi.org/10.1061/(ASCE)0733-9399(1990)116:3(565).

Deodatis, G. (1991). Weighted integral method. I: stochastic stiffness matrix. *117*(8), 1851-1864. https://doi.org/10.1061/(ASCE)0733-9399(1991)117:8(1851).

Elishakoff, I., & Ren, Y. (2003). *Finite element methods for structures with large stochastic variations* (Vol. 7). Oxford University Press, USA.

Elishakoff, I., Ren, Y.J., & Shinozuka, M. (1995). Some exact solutions for the bending of beams with spatially stochastic stiffness. *International Journal of Solids and Structures*, *32*(16), 2315-2327. https://doi.org/10.1016/0020-7683(94)00257-W.

Friedman, Z., & Kosmatka, J.B. (1993). Exact stiffness matrix of a nonuniform beam—II. Bending of a timoshenko beam. *Computers & Structures*, *49*(3), 545-555. https://doi.org/10.1016/0045-7949(93)90056-J.

Ghanem, R.G., & Spanos, P.D. (2003). *Stochastic finite elements: a spectral approach*. Courier Corporation, New York.

Grigoriu, M. (1993). On the spectral representation method in simulation. *Probabilistic Engineering Mechanics*, *8*(2), 75-90. https://doi.org/10.1016/0266-8920(93)90002-D.

Gurley, K.R., Tognarelli, M.A., & Kareem, A. (1997). Analysis and simulation tools for wind engineering. *Probabilistic Engineering Mechanics*, *12*(1), 9-31. https://doi.org/10.1016/S0266-8920(96)00010-0.

Häussler-Combe, U. (2022). *Computational structural concrete: theory and applications*. John Wiley & Sons, Germany.

Hien, T.D. (2020). A static analysis of nonuniform column by stochastic finite element method using weighted integration approach. *Transport and Communications Science Journal*, *71*(4), 359-367. https://doi.org/10.25073/tcsj.71.4.5.

Hien, T.D., Hung, N.D., Kien, N.T., & Noh, H.C. (2019). The variability of dynamic responses of beams resting on elastic foundation subjected to vehicle with random system parameters. *Applied Mathematical Modelling*, *67*, 676-687. https://doi.org/10.1016/j.apm.2018.11.018.

Huang, J., Yang, Q., Cao, H., & Ma, J. (2024). Structural reliability analysis using stochastic finite element method based on krylov subspace. *Algorithms*, *17*(10), 424. https://doi.org/10.3390/a17100424.

Huo, H., Yu, T., Zhao, J., Chen, G., & Yang, D. (2024). A novel uncertainty quantification method for determining deformations and reliabilities of stochastic laminated composite plates with geometric nonlinearity. *Computer Methods in Applied Mechanics and Engineering*, *420*, 116731. https://doi.org/10.1016/j.cma.2023.116731.

Johnson, E.A., Wojtkiewicz, S.F., Bergman, L.A., & Spencer, B.F. (1997). Observations with regard to massively parallel computation for Monte Carlo simulation of stochastic dynamical systems. *International Journal of Non-Linear Mechanics*, *32*(4), 721-734. https://doi.org/10.1016/S0020-7462(96)00097-2.

Kiureghian, A.D., & Ke, J.B. (1988). The stochastic finite element method in structural reliability. *Probabilistic Engineering Mechanics*, *3*(2), 83-91. https://doi.org/10.1016/0266-8920(88)90019-7.

Koh, K.J., & Cirak, F. (2023). Stochastic PDE representation of random fields for large-scale Gaussian process regression and statistical finite element analysis. *Computer Methods in Applied Mechanics and Engineering*, *417*, 116358. https://doi.org/10.1016/j.cma.2023.116358.

Larsen, M.L., Adhikari, S., & Arora, V. (2021). Analysis of stochastically parameterized prestressed beams and frames. *Engineering Structures*, *249*, 113312. https://doi.org/10.1016/j.engstruct.2021.113312.

Li, C.F., Feng, Y.T., Owen, D.R.J., & Davies, I.M. (2006). Fourier representation of random media fields in stochastic finite element modelling. *Engineering Computations*, *23*(7), 794-817. https://doi.org/10.1108/02644400610689901.

Liu, W.K., Belytschko, T., & Mani, A. (1986). Random field finite elements. *International Journal for Numerical Methods in Engineering*, *23*(10), 1831-1845. https://doi.org/10.1002/nme.1620231004.

Liu, X., Cao, Z.J., Li, D.Q., & Wang, Y. (2022). Adaptive Monte Carlo simulation method and its applications to reliability analysis of series systems with a large number of components. *Journal of Risk Uncertainty in Engineering Systems, Part A: Civil Engineering*, *8*(1), 04021075. https://doi.org/10.1061/AJRUA6.0001200.

Logan, D.L. (2022). *A first course in the finite element method*. 6th ed. Cengage Learning.

Matthies, H.G., & Keese, A. (2005). Galerkin methods for linear and nonlinear elliptic stochastic partial differential equations. *Computer Methods in Applied Mechanics and Engineering*, *194*(12), 1295-1331. https://doi.org/10.1016/j.cma.2004.05.027.

Nastos, C., Komninos, P., & Zarouchas, D. (2023). Non-destructive strength prediction of composite laminates utilizing deep learning and the stochastic finite element methods. *Composite Structures*, *311*, 116815. https://doi.org/10.1016/j.compstruct.2023.116815.

Nguyen, H.X., Ta, H.D., Lee, J., & Xuan, H.N. (2017). Stochastic buckling behaviour of laminated composite structures with uncertain material properties. *Aerospace Science and Technology*, *66*, 274-283. https://doi.org/10.1016/j.ast.2017.01.028.

Nouy, A. (2009). Recent developments in spectral stochastic methods for the numerical solution of stochastic partial differential equations. *Archives of Computational Methods in Engineering*, *16*(3), 251-285. https://doi.org/10.1007/s11831-009-9034-5.

Papadrakakis, M., & Kotsopulos, A. (1999). Parallel solution methods for stochastic finite element analysis using Monte Carlo simulation. *Computer Methods in Applied Mechanics and Engineering*, *168*(1), 305-320. https://doi.org/10.1016/S0045-7825(98)00147-9.

Popescu, R., Deodatis, G., & Nobahar, A. (2005). Effects of random heterogeneity of soil properties on bearing capacity. *Probabilistic Engineering Mechanics*, *20*(4), 324-341. https://doi.org/10.1016/j.probengmech.2005.06.003.

Ren, Y.J., Elishakoff, I., & Shinozuka, M. (1997). Finite element method for stochastic beams based on variational principles. *Journal of Applied Mechanics*, *64*(3), 664-669. https://doi.org/10.1115/1.2788944.

Schuëller, G.I. (2001). Computational stochastic mechanics – recent advances. *Computers & Structures*, *79*(22), 2225-2234. https://doi.org/10.1016/S0045-7949(01)00078-5.

Schuëller, G.I., & Pradlwarter, H.J. (2007). Benchmark study on reliability estimation in higher dimensions of structural systems – an overview. *Structural Safety*, *29*(3), 167-182.

Schuëller, G.I., & Pradlwarter, H.J. (2009). Uncertain linear systems in dynamics: retrospective and recent developments by stochastic approaches. *Engineering Structures*, *31*(11), 2507-2517.

Shao, Z., Li, X., & Xiang, P. (2023). A new computational scheme for structural static stochastic analysis based on Karhunen–Loève expansion and modified perturbation stochastic finite element method. *Computational Mechanics*, *71*(5), 917-933. https://doi.org/10.1007/s00466-022-02259-7.

Shinozuka, M., & Deodatis, G. (1991). Simulation of stochastic processes by spectral representation. *Applied Mechanics Reviews*, *44*(4), 191-204. https://doi.org/10.1115/1.3119501.

Shinozuka, M., & Deodatis, G. (1996). Simulation of multi-dimensional gaussian stochastic fields by spectral representation. *Applied Mechanics Reviews*, *49*(1), 29-53. https://doi.org/10.1115/1.3101883.

Stefanou, G. (2009). The stochastic finite element method: past, present and future. *Computer Methods in Applied Mechanics and Engineering*, *198*(9), 1031-1051. https://doi.org/10.1016/j.cma.2008.11.007.

Talib, S. (2024). Computational engineering advancements: general review of mathematical modelling in computer engineering applications. *Al-Rafidain Journal of Engineering Sciences*, *2*(1), 51-71.

Thakkar, B.S., & Karsh, P.K. (2025). Stochastic natural frequencies analysis of hybrid composites: a numerical approach. *Mechanics of Composite Materials*, *61*(1), 177-194. https://doi.org/10.1007/s11029-025-10269-8.

Thuan, N.V., & Hien, T.D. (2020). Stochastic perturbation-based finite element for free vibration of functionally graded beams with an uncertain elastic modulus. *Mechanics of Composite Materials*, *56*(4), 485-496.

Thuan, N.V., & Hien, T.D. (2021). Variablitity in frequencies of vehicle vibration anlysis with muiltiple random variables. *Transport and Communications Science Journal*, *72*(2), 215-226. https://doi.org/10.47869/tcsj.72.2.7.

Tripathy, R.K., & Bilionis, I. (2018). Deep UQ: learning deep neural network surrogate models for high dimensional uncertainty quantification. *Journal of Computational Physics*, *375*, 565-588.

Van den Nieuwenhof, B., & Coyette, J.P. (2003). Modal approaches for the stochastic finite element analysis of structures with material and geometric uncertainties. *Computer Methods in Applied Mechanics and Engineering*, *192*(33), 3705-3729. https://doi.org/10.1016/S0045-7825(03)00371-2.

Van Thuan, N., & Chun, N.H. (2019). The stochastic finite element in the natural frequency of functionally graded material beams. In *Mechanics of Functionally Graded Materials and Structures* (pp. 61). IntechOpen.

Wang, Q., Wu, D., Li, G., Liu, Z., Tong, J., Chen, X., & Gao, W. (2024). Machine learning aided uncertainty quantification for engineering structures involving material-geometric randomness and data imperfection. *Computer Methods in Applied Mechanics and Engineering*, *423*, 116868.

Xiu, D., & Karniadakis, G.E. (2002). The Wiener-Askey polynomial chaos for stochastic differential equations. *SIAM Journal on Scientific Computing*, *24*(2), 619-644. https://doi.org/https://doi.org/10.1137/S1064827501387826.

Zhang, J., & Ellingwood, B. (1994). Orthogonal series expansions of random fields in reliability analysis. *Journal of Engineering Mechanics*, *120*(12), 2660-2677. https://doi.org/10.1061/(ASCE)0733-9399(1994)120:12(2660).

Zhao, H., Zhang, Y., Zhu, W., Fu, C., & Lu, K. (2024). A comprehensive study on seismic dynamic responses of stochastic structures using sparse grid-based polynomial chaos expansion. *Engineering Structures*, *306*, 117753.